

Intensive steel quenching processes taking place in liquid media that are considered from the point of view of modern physics

Nikolai Kobasko

PhD, Fellow of ASM International, Intensive Technologies Ltd, 68/1 Peremohy Ave, Kyiv, Ukraine

Abstract

In the paper the physics of quenching the large steel components in water salt and polymer solutions are considered. It is shown that during immersion of steel samples into cold solution cooling process is intensive if any film boiling is completely absent. In this case martensite start temperature M_s should prevail saturation temperature T_s , *i.e.* $M_s > T_s$. Mechanism of creation a “shoulder” on the surface cooling curve during quenching in 18% water PAG solution is explained by existence of the self – regulated thermal process on the insulated layer and variation of its thickness. Obtained results of investigations are recommended to use for quenching recipes development and performing austempering processes via cold liquids to improve cardinal service life of hardened steel components. It is underlined in the paper that further progress in the field can be done if efforts of physician, mathematician and experts from heat treating industry are combined. Obtained results can be useful for practice and further scientific investigations.

Keywords: large samples, IQ process, physics of “shoulder”, austempering, cold liquid, benefits

1. Introduction

As known, according to author (Tensi, 1992) ^[1], the following four possible scenarios of heat transfer on the probe surface takes place during quenching cylindrical probes in liquid media:

- Full film boiling and nucleate boiling are present at the same time on the probe surface. The area of nucleate boiling moves up along the probe surface replacing film boiling. Wetting process of a cylindrical Cr-Ni steel sample (15 mm in diameter and 45 mm long) being quenched in water of 60°C without agitation is discussed in the book^[1].
- First, film boiling takes place throughout the entire probe surface area. At a certain point in time, nucleate boiling replaces film boiling and then convection heat transfer replaces nucleate boiling that is well known a classical consideration^[1,2].
- Some local areas of the probe surface are covered by the vapor blanket, while at the same time, other areas experience nucleate boiling. These local areas do not move and are reason for big distortion of steel parts during quenching in liquid media^[1,3].
- The boiling process takes place on some local areas of the probe surface. Film boiling and nucleate boiling appear periodically in these areas, replacing each other (see Fig. 2) ^[1, 4].

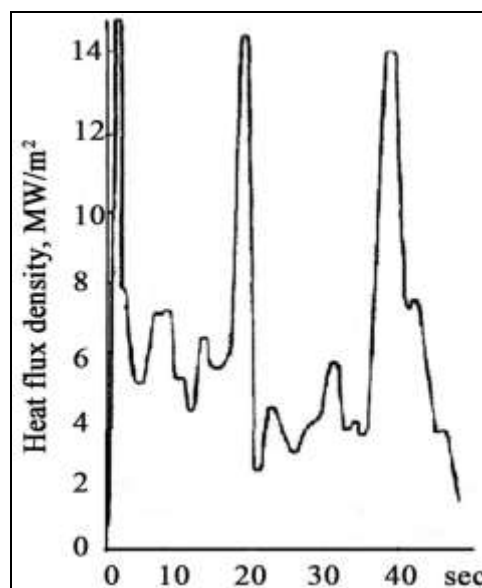


Fig 1: Periodic changes of heat flux density versus time during quenching of a cylindrical probe made of AISI 304 steel in 0.3% water solution of polyoxyethylene at 20°C (probe diameter 20 mm, length 80 mm, initial temperature 850 °C). Periodic changes are explained by multiple transitions from film boiling to nucleate boiling ^[4].

Four scenarios of heat transfer on the probe surface was explained from the point of view of relationship between initial and critical heat flux densities in the published paper [5]. More information on mentioned phenomena one can find in the published literature [6, 7].

This paper considers the process of large probes quenching in water salt solutions of optimal concentration and polymer water solutions which are slowly agitated to see whether process of cooling in considered condition could be very intensive. It is assumed that any film boiling is absent and only transient nucleate boiling and convection takes place during quenching. Absence of film boiling is explained by existence double electrical layer which provides maximal critical heat flux density during quenching in optimal concentration of water salt solutions [8, 9].

Absence of film boiling during quenching in water polymer solutions of inverse solubility is explained by immediate creation of surface insulating layer [10, 12]. Due to presence a thin insulating layer, initial heat flux density drops below its critical value preventing effectively any film boiling (see Fig.2) [11].

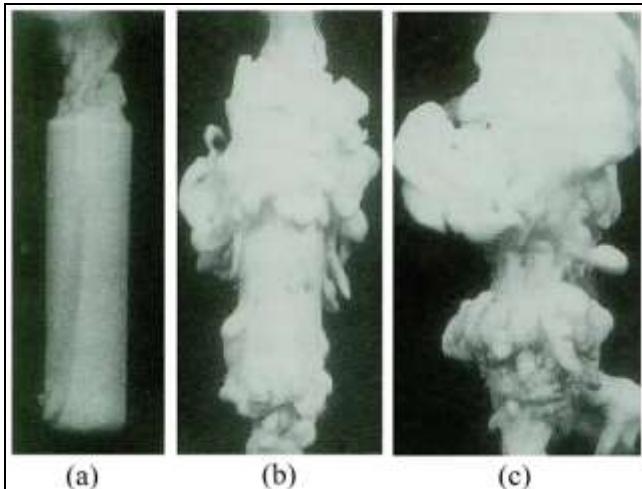


Fig 2: Immediate formation of insulating layer during cooling cylindrical silver probe 15 mm in diameter and 45 mm long in water solution of inverse solubility polymer at 25 °C^[11]: a – 6 sec; b – 6.35 sec; c – 7.65 sec.

The decrease of initial heat flux density q_0 is calculated by Eq. (1):

$$q_{in} = \frac{q_0}{\left(1 + 2 \frac{\delta}{R} \frac{\lambda}{\lambda_{coat}}\right)} \quad (1)$$

The new approach requires new technique for investigating mechanism of insulating layer formation, taking into accounts its thickness variation and thermal properties of insulating material to properly investigate such processes. Intensity of cooling in this case, as known, is provided by dimensionless number Kn [4, 5]. Optimal hardened layer during cooling in any condition is achieved if Eq. (2) is satisfied [6, 7]:

2. Mathematical model for solving direct and inverse problem during quenching

Mathematical model for calculating direct and inverse problem (temperature field, heat flux densities and heat transfer coefficients calculation during quenching of steel components in liquid media) should include hyperbolic heat conductivity equation (2), boundary condition (3) and initial condition (4). In last decade, direct and inverse problem for hyperbolic heat conductivity equation were considered and solved by physicians and mathematicians [13, 16].

$$c\rho \frac{\partial T}{\partial \tau} + r \cdot \frac{\partial^2 T}{\partial \tau^2} = \text{div}[\lambda(T) \text{grad}T] + cL_c \frac{\partial P}{\partial T} \cdot \frac{\partial T}{\partial \tau} \quad (2)$$

Here c is specific heat capacity; ρ is density; r is relaxation time; λ is thermal conductivity of material; L_c is a specific thermal effect of phase transformation in solid material during its quenching; P is a volume fraction of the structural component in solid alloy during quenching; τ is time; T is temperature.

The value of P depends on type of phase transformation and is constructed by use isothermal or cooling continuous transformation diagrams. One can find useful information on this subject in publication of authors [17]. For example, if isothermal kinetics of austenite decomposition occurs according to Eq. (2a), then P is a volume fraction of the structural component in steel.

$$P(\tau) = 1 - \exp[-K_1(T) \cdot \tau^{n(T)}] \quad (2a)$$

In Eq. (2a), K_1 and n are determined from TTT (time-temperature –transformation) diagram.

As a rule, the first type of boundary condition is recorded by accurate experiments using surface thermocouples and is written as:

$$T_{sf} = f(\tau) \quad (3)$$

Currently, Ukrainian scientists are considering boundary condition taking into account a double electrical layer which is a reason for existence thermal waves during quenching of steel [13].

Initial condition for quenching steel components from austenitizing temperature in liquid media is simple because at the beginning of cooling temperature through section of steel component is the same, *i.e.*:

$$T(x, y, z, 0) = T_0 \quad (4)$$

Since during transformation austenite into martensite thermal effect of transformation is insignificant and relaxation time r is extremely small value, the Eq. (2) can be reduced to more simple parabolic form (5):

$$C_{eff} \frac{\partial T}{\partial \tau} = \text{div}[\lambda(T) \text{grad}T] \quad (5)$$

Here $C_{eff} = \rho \left(c + L_c \frac{\partial \mathcal{P}}{\partial T} \right)$

It is possible to do so because transient nucleate boiling formation requires some time after which parabolic heat conductivity equation starts to govern cooling process. In literature there are accurate experimental data recorded and published by French who quenched spherical steel samples of different diameters from 875°C in 5% water solution of NaOH at 20°C with agitation 0.914 m/s (see Table 1)^[18].

Table 1: Time required for the surface of steel sphere 120.6 mm in diameter to cool to different temperatures when quenched from 875°C in 5% water solution of NaOH at 20°C and moving at 0.914 m/s^[18].

Size, inches (m)	Time, sec							
	700°C	600°C	500°C	400°C	300°C	250°C	200°C	150°C
	0.040	0.070	0.11	0.13	0.15	0.17	0.28	1.60
4.75"	0.050	0.065	0.08	0.12	0.19	0.24	0.35	1.10
(0.1206)	0.040	0.062	0.09	0.12	0.18	0.23	0.32	0.78
	0.042	0.065	0.08	0.12	0.24	0.27	0.35	0.60
Average	0.043	0.066	0.09	0.12	0.17	0.21	0.29	0.95

According to French^[18], surface cooling curves within initial temperature T_0 and start temperature of transient nucleate boiling process are almost the same and they don't depend on form and size of steel part if film boiling is completely absent. It is explained by extreme processes taking place during quenching without film boiling mode resulting in their very short time. Within this short time, very thin quenched surface layer is formed which initially can be considered as an unbounded thin plate for all form of samples. French provided experimental data only for interval of temperatures 875°C – 150°C (see Table 1). Using experimental data of French, transient nucleate boiling process was reconstructed by author of this paper based on recently published investigations^[19]. It was assumed that samples of spherical, cylindrical and plate like forms have thickness 120 mm which were quenched in water salt solutions at 20°C without creating film boiling process and agitation of liquid was 0.5 m/s. Also, experimental data which were recently published by German scientists were used who investigated cooling processes in water polymer solutions of polyalkylene glycol (PAG) at 23°C^[20]. Especially interesting are experimental data of authors^[20] regarding large sample (150 mm in diameter and 580 mm long) which was quenched in 18% water solution of PAG (see Fig. 2). The aim of current investigation is finding out whether intensive quenching can be performed in slow agitated water solutions and become less costly due to eliminating powerful pumps and rotating impellers. It is very important to know whether austempering process via cold liquids is possible for large steel components. Results of computer modeling, using above mentioned experimental data and software IQLab which explores Eq. (5) with boundary condition (3) and

Initial condition (4), are discussed below^[21].

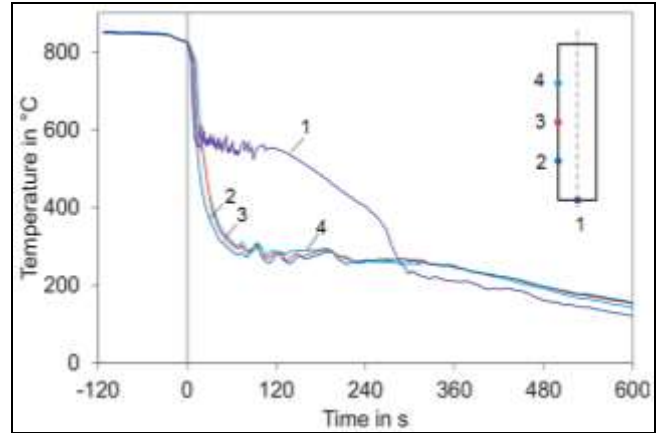
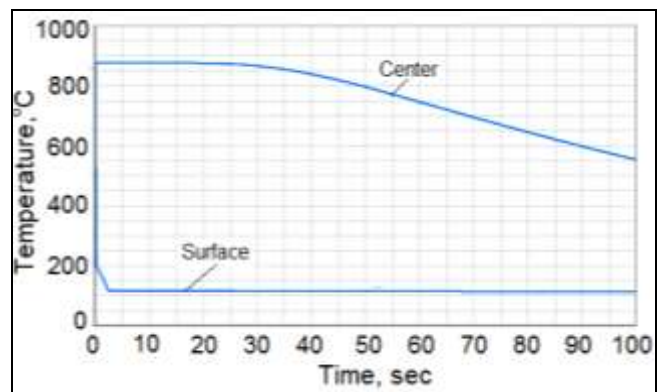


Fig 3: Cooling curves of a shaft (150 mm diameter, 580 mm long and 78 kg mass) quenched in an industrial quench tank filled with 18% water solution of PAG solution. Colored spots indicate schematically the measuring positions^[20].

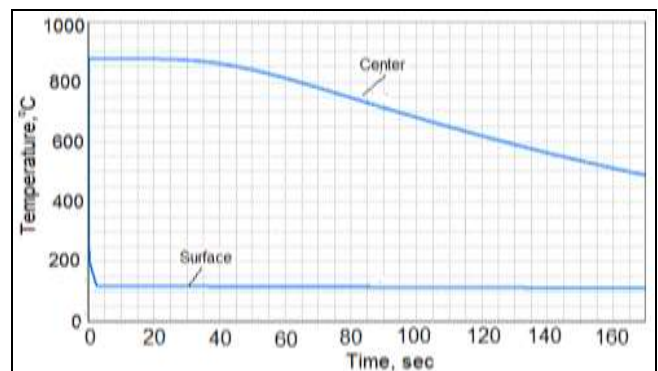
As seen from Fig. 3, there is a film boiling at the bottom of shaft which was recorded by thermocouple 1. There was no film boiling in areas where thermocouples 2, 3, and 4 were located. This issue is discussed at the end of this paper.

2.1 Numerical temperature cooling curves calculation during quenching of large steel samples in water solutions

Numerical computer calculations of temperature fields show forming of huge temperature gradients during immersion of steel samples into cold liquid in case of film boiling absent.



(a)



(b)

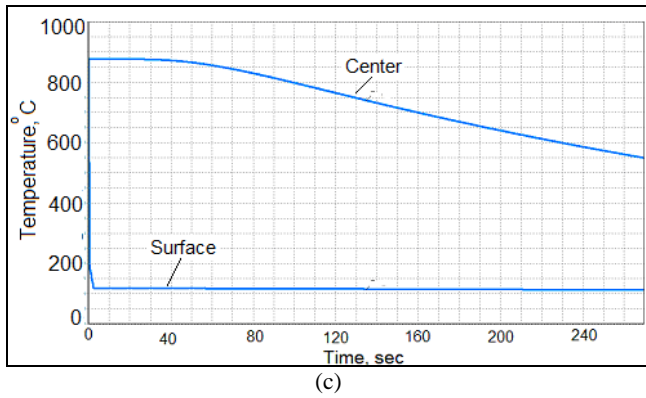


Fig 4: Surface and core cooling curves versus time during quenching steel samples of classical forms in water salt solutions of optimal concentration at 20°C with agitation 0.5 m/s: a), spherical sample 120 mm diameter; b), cylindrical sample 120 mm diameter; c), plate 120 mm thickness.

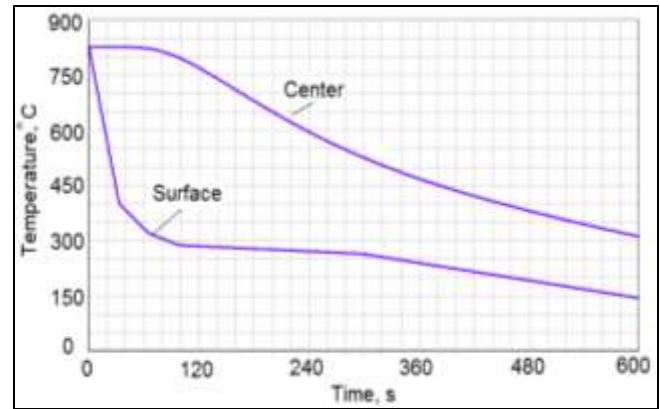


Fig 5: Surface and core cooling curves versus time during quenching the shaft (Ø 150 mm, 580 mm length, 78 kg mass) in an industrial quench tank filled with 18% water PAG solution as it follows from the computer modeling.

Measurements of the surface temperature during quenching of a shaft (Ø 150 mm, 580 mm length, 78 kg mass) in an industrial quench tank filled with 18% water PAG solution are presented in Fig. 3^[20]. Using experimental measurement of authors^[20], the core temperature of the shaft (Ø 120 mm, 580 mm length, 78 kg mass) was reconstructed by computer modeling (see Fig. 5).

It appeared that core temperature at the end of shoulder (moment of time 300 sec) during quenching shaft with thickness 150 mm in water PAG solution is about 525°C. During intensive quenching of classical samples with thickness 120 mm in water salt solutions at 20°C and agitation 0.5 m/s, core temperature at the end of transient nucleate boiling process is 540°C (see Table 2).

Table 2: Duration of nucleate boiling (NB) and surface-core temperature at its end for different sizes and forms of samples.

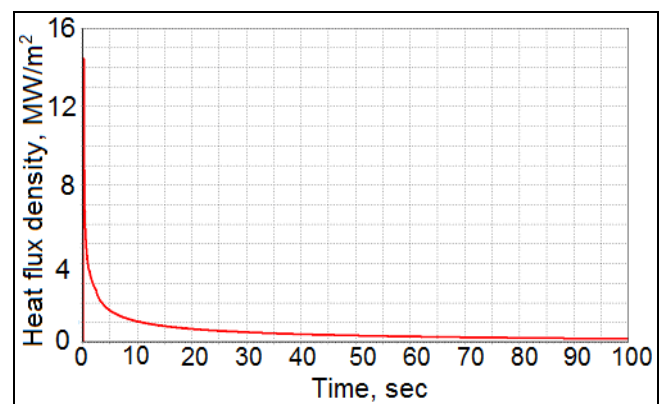
Size and form of sample, mm	Duration of NB, sec	Surface temperature at the end of NB, °C	Core temperature at the end of NB, °C
Sphere, 120	100	112	550
Cylinder, 120	170	112	540
Plate, 120	270	112	540
Cylinder, 150 Quenching in PAG solution	300	263	525

Such strange difference is explained by effect of insulating layer of low thermal conductivity and by reduced convective heat transfer coefficient due to increased viscosity of water polymer solution. In any event, results of calculations show the possibility to perform austempering process via cold liquids and significantly improve strength of material. This problem is considered below.

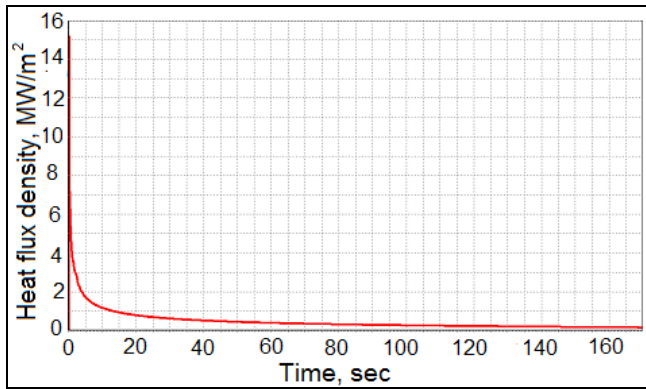
This type of heat transfer mode, Tensi called this type of heat transfer the third type of heat exchange during boiling which is discussed in the introduction of current paper^[1]. This type of heat transfer is the most dangerous because local film boiling results in high distortion of steel parts during quenching and in many cases generates quench crack formation.

2.2 Numerical heat flux densities calculation during quenching of large steel samples

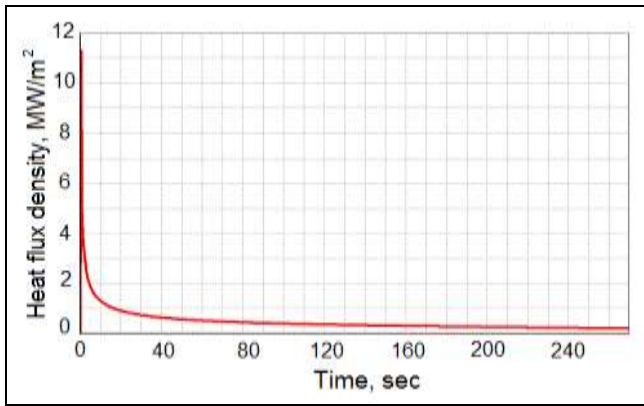
The heat flux density is calculated with aim of prediction film boiling process during quenching of steel parts. If initial heat flux density is larger than the first critical heat flux density q_{cr1} , then full film boiling takes place during quenching in liquid media. If initial heat flux density is below the first critical heat flux density q_{cr1} , then any film boiling during quenching of steel parts in liquid media is absent. If initial heat flux density is equal to the first critical heat flux density q_{cr1} then local film boiling on the surface of steel parts takes place during quenching in liquid media.



(a)



(b)



(c)

Fig 6: Heat flux density versus time during quenching samples of classical forms 120 mm in diameter in water salt solution of optimal concentration at 20°C when film boiling is absent: a), spherical form; b), cylindrical form: c), plate.

Summarizing results of calculations are presented in Table 3.

Fig 3: Heat flux densities for different sizes and forms of investigated samples

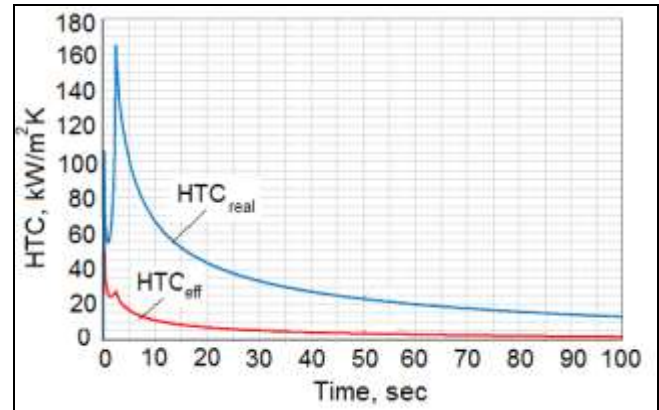
Size and form of sample, mm	Max initial heat flux density in MW/m ²	Heat flux density in MW/m ² after 10% of NB	Heat flux density in MW/m ² at the end of NB
Sphere	14.4	1.0	0.15
Cylinder	15.2	0.8	0.20
Plate	11.4	0.75	0.20 – 0.25

It is shown that initial heat flux densities q_{in} can be easily dropped below q_{cr1} by creation a thin insulating later on the surface of steel parts during their quenching [10, 12].

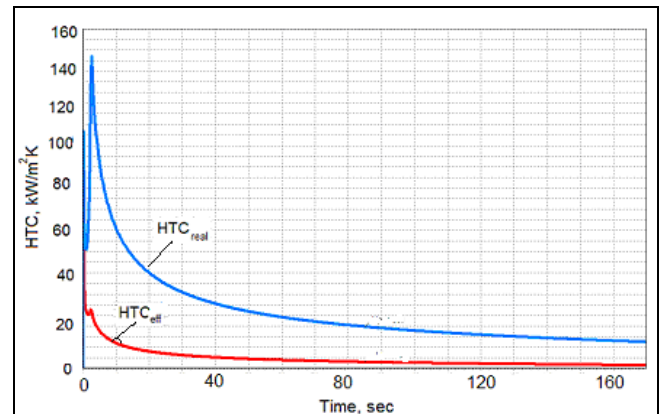
2.3 Numerical calculation of real and effective HTC's during quenching of large steel samples in liquid media

The real heat transfer coefficient (HTC) is responsible for creation temperature gradients in quenched steel parts. It is well known that HTC provides via Biot number Bi the degree of temperature smoothness through section of quenched steel part during its hardening. If $Bi < 0.2$, it is assumed that surface temperature is approximately equal to core temperature during quenching of steel part. That is true only for real HTC and not is true for effective HTC. The real HTC relates to overheat of a boundary layer $T - T_s$ while effective HTC relates to

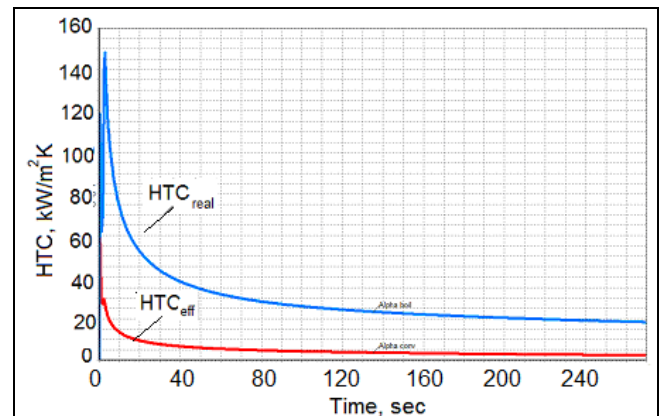
underheat plus overheat during quenching. When Biot number Bi is calculated using effective HTC, the big error in many cases arises due to $T - T_s \ll T - T_m$. Historically, effective HTC's are widely used in heat treating industry. They should be considered as the empirical values which can work for cooling time and cooling rate calculations. Real and effective HTC's versus time during quenching samples of classical forms 120 mm in diameter in water salt solution of optimal concentration at 20°C when film boiling is absent are presented in Fig. 7



(a)



(b)



(c)

Fig 7: Real and effective HTC's versus time during quenching samples of classical forms 120 mm in diameter in water salt solution of optimal concentration at 20°C when film boiling is absent: a), spherical form; b), cylindrical form: c), plate.

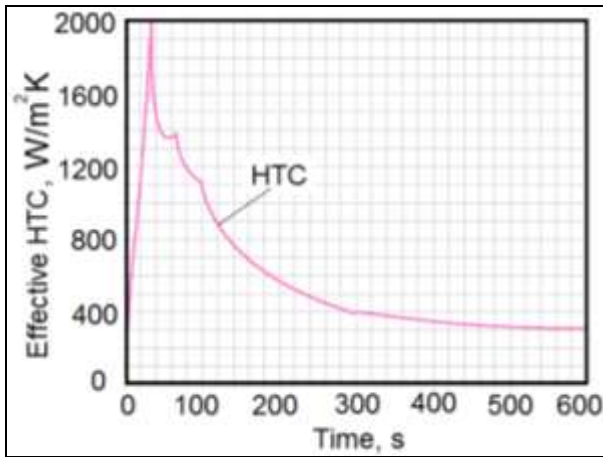


Fig 8: Effective HTCs versus time during quenching shaft (ϕ 150 mm, 580 mm length, 78 kg mass) in an industrial quench tank filled with 18% water PAG solution.

It is typical graphs of transient nucleate boiling process when surface of metal is covered by insulating layer. Table 4 summarizes investigations of HTCs for classical forms concerning their maximal values.

Table 4: Maximal real and effective HTCs for different sizes and forms of investigated samples

Size and form of sample, mm	Max real HTC in kW/m ² K	Max effective HTC in kW/m ² K
Sphere	165	27
Cylinder	148	25
Plate	148	24

It is clearly seen from Table 4 that real HTC is larger more than 6 times as compared with the effective HTC.

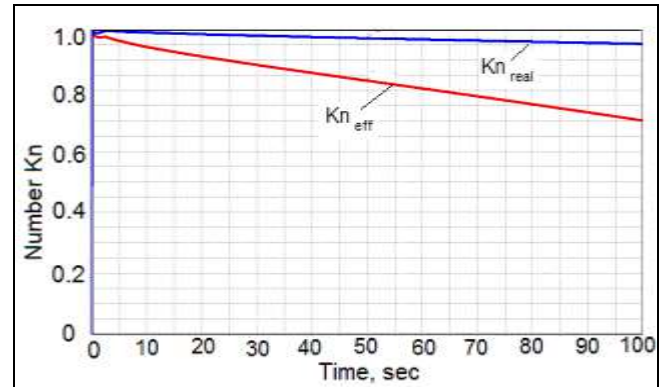
2.4 Numerical Kondrat’ev numbers Kn calculation during quenching of large steel samples

Kondrat’ev numbers Kn were calculated during computer modeling of the quenching process using Eq. (6) [27]:

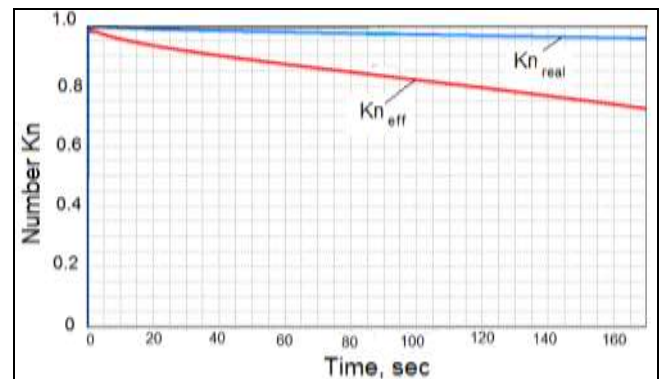
$$Kn = \frac{Bi_v}{(Bi_v^2 + 1.437Bi_v + 1)^{0.5}} \quad (6)$$

Results of calculations have a practical value since they allow recipes development, cooling rate evaluation and microstructure prediction at the core of steel parts of any configuration [28].

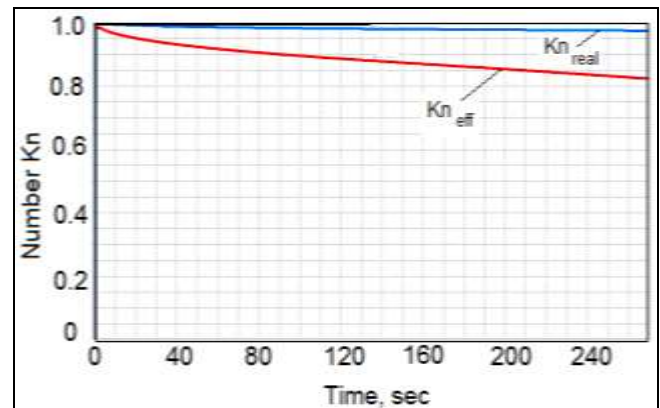
Results of performed calculations are presented in Fig. 9.



(a)



(b)



(c)

Fig 9: Real and effective dimensionless Kondrat’ev numbers versus time during quenching samples of classical forms 120 mm in diameter in water salt solution of optimal concentration at 20°C when film boiling is absent: a), spherical form; b), cylindrical form; c), plate.

Similar calculations were fulfilled for large shaft using experimental data of authors [20] (see Fig. 10).

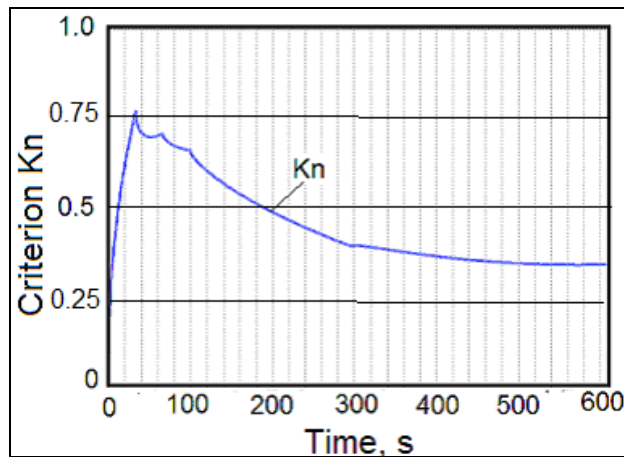


Fig 10: Effective dimensionless Kondrat'ev numbers Kn versus time during shaft (ϕ 150 mm, 580 mm length, 78 kg mass) in an industrial quench tank filled with 18% water PAG solution.

Table 5 summarizes investigations of dimensionless numbers Kn for classical forms concerning their maximal values.

Table 5: Real and effective Kondrat'ev numbers Kn for classical forms 120 mm in thickness during quenching in water salt solution of optimal concentration at 20°C when film boiling is absent.

Form of sample, mm	Real or effective Kn	Max Kn	Kn at the end of NB	Average value
Sphere	Real	1	0.94	0.97
	Effective	0.98	0.70	0.84
Cylinder	Real	1	0.95	0.975
	Effective	1	0.83	0.915
Plate	Real	1	0.94	0.97
	Effective	1	0.824	0.912

Table 5 shows that quenching was intensive because Kn numbers $Kn > 0.8$. It was agreed to consider intensive

quenching when Kn number is within $0.8 < Kn < 1$ ^[3].

3. Effect of accelerated cooling on improving mechanical properties of steel at the core of machine components

Obtained results of calculations can be used to predict hardness and microstructure at the core of quenched steel parts^[28]. For this purpose the cooling rate is evaluated using Eq. (7).

$$v = \frac{aKn}{K} (T - T_m) \tag{7}$$

Cooling rate for cylindrical specimens 50 mm in diameter quenched in water salt solution of optimal concentration are provided in Table 6.

Table 6: Cooling rate V at the core of cylindrical specimen (50 mm diameter) at a temperature 705°C when quenching in oil and water salt solutions agitated with 0.5 m/s.

Quenchant	Kn	K	$T - T_m$	V
Oil at 60°C	0.20	$108 \times 10^{-6} m^2$	640°C	6.4°C/s
Agitated water Solution 20°C	0.82	$108 \times 10^{-6} m^2$	680°C	28°C/s

Comparing obtained cooling rate with the cooling rate in Jominy test (see Table 7), it is possible to predict microstructure, hardness and mechanical properties of

material at the core of quenched machine components (see Table 8). More information on this subject one can find in a book^[28].

Table 7: Cooling rate at 705°C (1300°F) in a Jominy specimen as a function of distance from quenched end^[29].

Distance from water –quenched end, 1.6 mm (1/16 inch)	Cooling °C/s	Rate °F/s
1	270	480
2	170	305
3	110	195
4	70	125
5	43	77
6	31	56
7	23	42
8	16	33
9	14	26

10	11.9	21.4
12	9.1	16.3
14	6.9	12.4
16	5.6	10
18	4.6	8.3
20	3.9	7

Table 8: Mechanical properties at the core of cylindrical probes 50 mm in diameter made of different steels and quenched in oil and water salt solutions [30].

Steel grade	Quenchant	R _m (MPa)	R _{p0.2} (MPa)	A (%)	Z (%)	a _k (J/cm ²)	HB
AISI	Oil	950	775	14	53	54	285
4135 (35KhM)	Water salt solution	970	820	17	63	150	285
AISI	Oil	770	575	23	64	13.8	217
4140 (40Kh)	Water salt solution	860	695	16.5	65	168	269

Table 8 shows improvement of mechanical properties at the core of cylindrical probes 50 mm in diameter made of different steels and quenched in oil and water salt solutions [30].

4. Discussion

According to law of conservation of physics, heat flux densities in the area of transition from metal to insulating layer are always equal and can be written as:

$$q_{in} = q_{st} \tag{8}$$

Heat flux density is calculated by law of Fourier $q = \lambda gradT$ that is why true equines (9) is

$$\lambda_{in} gradT_{in} = \lambda_{st} gradT_{st} \tag{9}$$

Which can be rewritten as:

$$\frac{\lambda_{in}}{\lambda_{st}} = \frac{gradT_{st}}{gradT_{in}} \tag{10}$$

It means that temperature gradient in the insulating layer is larger as compared with the temperature gradient in steel because

$$\lambda_{st} \gg \lambda_{in} \tag{11}$$

Since transient nucleate boiling process takes place on the surface of insulating layer, it means that insulating surface temperature during nucleate boiling process, according to investigation [3, 9], is fixed at the level of

$$T_{sf} = T_s + \Delta \bar{\xi} \approx Const \tag{12}$$

Here λ_{in} is thermal conductivity of material that creates insulating layer; λ_{st} is thermal conductivity of steel; $gradT_{in}$ is

temperature gradient in the insulating layer; $gradT_{st}$ is temperature gradient in steel sample; T_{sf} is surface temperature; T_s is saturation temperature; $\Delta \bar{\xi}$ is overheat of boundary layer that is responsible for transient nucleate boiling process.

Statement (12) was supported by accurate experiments carried out in Ukraine, USA and Japan [3, 22, 23].

From the point of view of physics of the boiling process, insignificant changing of surface temperature during nucleate boiling is explained by well know relationship between heat flux density and overheat of the boundary layer (see Eq. (13)). Heat flux density is proportional to cube of the overheat of a boundary layer [24], i.e.:

$$q \propto (\Delta \bar{\xi})^3 \tag{13}$$

A small change in overheating layer results in huge change of heat flux density q (see Eq. (13)). That is a reason for maintaining the surface temperature during transient nucleate boiling process at the saturation level.

Proceeding from above mentioned, it possible to explain very important experimental results obtained recently by scientists from Germany [20] concerning cooling large shaft (150 mm diameter and 580 mm length) in 18% water polymer solution of PAG (see Fig. 3). Authors [20] explained obtained results of experiment on the basis of periodical changing of film boiling process that takes place during quenching. Some evidences show that it cannot be film boiling process and such evidences are:

- The average Kondrat'ev number Kn for shaft 150 mm diameter which was quenched in 18% water PAG solution is 0.6 (within interval of time 0 - 200 sec) while during film boiling it can be only 0.14.
- Frequency of surface temperature varying is rather low while frequency of surface temperature generated by film boiling is much higher.
- Surface cooling curves recorded by thermocouples 2, 3, and 4 are stable while film boiling process produces unstable cooling curves.
- Effective heat transfer coefficient (HTC) within interval of time 0 -200 sec varies from 500 W/m²K to 2000 W/m²K while during film boiling process it should vary within 150 W/m²K – 300 W/m²K.
- All three cooling curves, recorded by thermocouples 2, 3, and 4, within the interval of time 40 sec – 300 sec create a shelf which looks like “shoulder” and is rather stable (see Fig. 3). Any film boiling cannot provide such result.

These five differences can be easily explained using equations (10) – (13).

The average Kondrat'ev number Kn is relatively large because film boiling in areas where three thermocouples 2, 3, and 4 were located was completely absent. Certainly, dimensionless number Kn is reduced to $Kn = 0.6$ because surface temperature of large probe was maintaining a long time approximately at the level of 300°C (see Fig. 3 and Table 9).

Table 9: Kondrat'ev numbers Kn and cooling rate at 705°C of investigated cylindrical samples during quenching

Form and size of probe in mm	Kn	$V, ^{\circ}\text{C/s}$
Sphere 120	0.83	8.4
Cylinder 120	0.84	5
Plate\120	0.87	2.1
Shaft 150	0.60	2.3

The varying of surface temperature with a low frequency is explained by varying thickness of the insulating layer during quenching of large shaft. According to Eq. (10), when thickness of insulating layer decreases, surface temperature of steel increases because surface temperature on insulating layer is fixed. In opinion of the author of current paper, varying surface temperature of shaft is connected with the varying of

thickness of insulating later during quenching process.

Cooling curves during transient nucleate boiling process are stable because film boiling was completely absent and nucleate boiling always provides uniform and accelerated quenching [11, 12].

Effective HTC during quenching shaft in PAG solution is within $500 \text{ W/m}^2\text{K} - 2000 \text{ W/m}^2\text{K}$ due to existence thermal resistance provided by insulating layer.

Stability of a shoulder (shelf) on the cooling curve during quenching shaft in water polymer solution is explained by stability of nucleate boiling process on the insulated surface layer.

The obtained experimental results have a great value instead of existence a difference in their explanation [20]. It is completely clear that austempering process via cold liquid for large steel components can be successfully performed. The idea on performing austempering processes via cold liquids was for the first time forwarded in Ukraine [25] and is widely discussed in the recently published book [26]. As an example, let's consider CCT diagram shown in Fig. 11 to see how austempering process via cols liquid is performed.

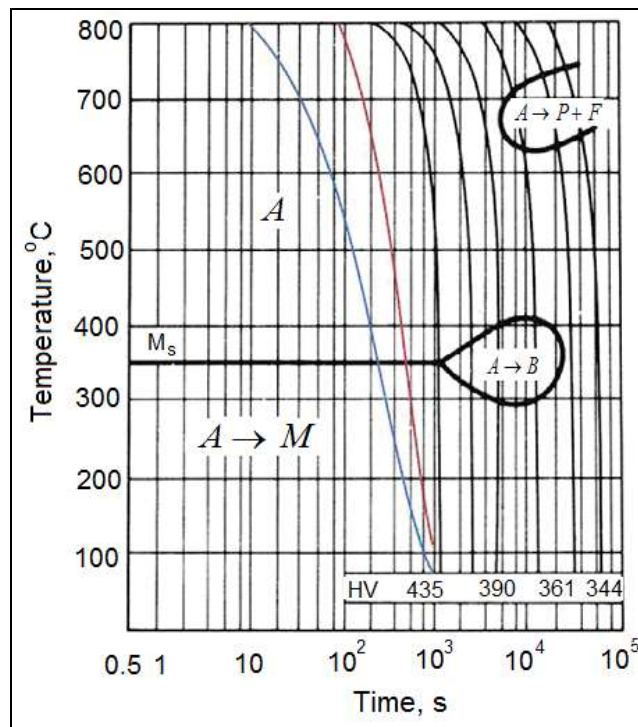


Fig 11: Cooling continuous transformation (CCT) diagram for steel 25Kh5MF used for performing austempering process via cold liquid [31, 32]: A is austenite; B is bainite; P is pearlite; F is ferrite; M is martensite.

More information on new technology one can get from the literature [25, 26, 33]. It is rather simple if martensite transformation during quenching is delayed (see Fig. 3). If shaft 150 mm in diameter is made of steel 25Kh5MF, cooling during its quenching in 18% water polymer PAG solution should be interrupted at a time 300 seconds in put immediately for tempering at a temperature 350°C or a little bit higher. In this case bainitic microstructure is formed through section of the shaft, providing high ductility and

strength of the hardened steel. Detail information on bainitic transformations is widely and deeply discussed in the book [34].

Along with the austempering process via cold liquids, optimized bainitic transformation can be used during intensive quenching which is called direct convection or IQ-3 technological process [35]. In this particular case, very intensive quenching should be interrupted at proper time and provide immediate tempering at a temperature that results in

high strength bainitic structure formation at the core of quenched steel parts. Such modified technology increases cardinal service life of quenched machine components due to high surface compression residual stresses in surface layers and ductility and strength of material at the core of machine components.

5. Conclusions

1. Intensive quenching process can be performed in water salt solutions or low concentration of PAG solutions through complete elimination of film boiling during quenching, In this case martensite start temperature M_s - should prevail saturation temperature T_s , *i.e.* $M_s > T_s$.
2. Core temperature of different forms and rather large samples (120 – 150 mm of thickness) during quenching in water solutions of low concentration with agitation 0.5 m/s at the end of transient nucleate boiling process is at the level of 525°C – 550°C. It can be used for calculating transition from nucleate boiling to convection when developing recipes of hardening processes.
3. The physics of creation of a “shoulder” in surface temperature cooling curves during stable transient nucleate boiling process on the surface of large samples is explained considering the effect of insulating polymeric layer and its variation on surface temperature during quenching. Findings can be used for performing austempering process via cold liquids for different form and sizes of steel parts (up to 150 mm in thickness).
4. Quenching processes, which are very complicated, have to be considered from the point of view of modern physics including crisis of boiling taking place in liquid media. The hyperbolic heat conductivity equation should be considered in this case taking into account existence of double electrical layer when quenching in water salt solutions. At present the problem with the double electrical boundary condition is not considered yet. It can be done in the nearest future combining efforts of physicians, mathematicians and experts working in heat treating industry.

References

1. Tensi HM. Wetting Kinematics. Handbook “Theory and Technology of Quenching”. Springer-Verlag, Berlin, 1992, 208-219.
2. Totten GE and Tensi HM. Using Conductance Data to Characterize Quenchants. Heat Treating Progress. 2002; 2(5):39-42.
3. Kobasko NI, Aronov MA, Powell JA, Totten GE. Intensive Quenching Systems: Engineering and Design. ASTM International, USA, 2010, 234. doi: 10.1520/mnl64-eb
4. Kobasko NI, Krivoshei FA. On the Mechanism of Temperature and Heat Flow Oscillations in Cooling Metallic Specimens in Aqueous Solutions of Polymers. Dokl. Akad. Nauk Ukr, 1994; 11:90-94.
5. Kobasko NI. Current State of the Problem and Principal Criteria to Evaluating the Cooling Capacity of Quenching Media. Metal Science and Heat Treatmen. 1996; 38(1-2):49-55.
6. Vergana-Hernandez HJ, Hernandez-Morales B. A Novel Probe Design to Study Wetting Front Kinematics During Forced Convective Quenching, Experimental. Thermal and Fluid Science. 2009; 33(5):797-807.
7. Krivoshei FA. Solution of Inverse Problems of Heat Transfer Based on the Method of Statistical Regularization. Author’s abstract of doctoral thesis (in Russian), Kyiv, 1993.
8. Frenkel YaI. Kinetic Theory of Liquids. Nauka, Leningrad, 1975.
9. Kobasko NI. Steel Quenching in Liquid Media Under Pressure. Naukova Dumka, Kyiv, 1980, 206.
10. Kobasko NI. High Quality Steel vs Surface Polymeric Layer during Quenching. Lambert Academic Publishing, Germany, 2019, 102. ISBN: 978-613-9-45596-6.
11. Kobasko NI. Uniform and Intense Cooling During Hardening Steel in Low Concentration of Water Polymer Solutions. American Journal of Modern Physics. 2019, 8(6):76-85. doi: 10.11648/j.ajmp.20190806.11
12. Kobasko NI. Uniform and Intense Cooling During Hardening Steel in Low Concentration of Water Polymer Solutions. In: Ibtissem BELGACEM, editor. Prime Archives in Physics. Vide Leaf, Hyderabad, India, 2020, 27.
13. Kobasko NI. Thermal Waves, Thermal Diffusivity and Possibility of Relaxation Time of Materials Evaluation. SSRG International Journal of Applied Physics (SSRG-IJAP). 2019; 6(3):66-73.
14. Guseynov ShE, Buikis A, Kobasko NI. Mathematical statement of a problem with the hyperbolic heat conductivity equation for the intensive quenching processes. Proc. of the Seventh International Conference “Equipment and Technologies for Heat Treatment Metals and Alloys (OTTOM-7)”. Kharkov, Ukraine, 2006; 2:22-27.
15. Guseynov ShE, Rimshans JS, Kobasko NI. On one non – linear mathematical model for intensive steel quenching and its analytical solution in closed form. Progress in Industrial Mathematics at ECMI (Mathematics in Industry 15), Fitt AD, *et al.* (Eds.). Springer – Verlag, Berlin, Heidelberg, 2010, 857-862.
16. Buikis A. Multidimensional mathematical models for intensive steel quenching. Lambert Academic Publishing, Germany, 2020, 128.
17. Reti T, Felde I, Grum J, *et al.* Extension of Isothermal Time-Temperature Parameters to Non-isothermal Conditions: Application to the Simulation of Rapid Tempering. Strojnicki Vestnik. 2010; 56(2):84-92.
18. French HJ. The Quenching of Steels, American Society for Steel Treating, Cleveland, OH, 1930.
19. Kobasko NI. Intensive Quenching Technology Accuracy Analysis Based on Study Physics of Transient Nucleate Boiling Process. SSRG International Journal of Applied Physics. 2020; 7(1):27-35.
20. Waldeck S, Castens M, Riefler N, Frerichs F, Luebben Th, Fritsching U, *et al.* Mechanisms and Process Control for Quenching with Aqueous Polymer Solutions. HTM J. Heat Treatm. Mat. 2019; 74(4):1-19. DOI:10.3139/105.110387.
21. Kobasko NI, Dobryvechir VV. Inverse Problems in

- Quench Process Design. In a Book “Intensive Quenching Systems: Engineering and Design”. ASTM International, W. Conshohocken, USA, 2010, 210-229.
22. Kobasko NI. Thermal Processes in Quenching of Steel. *Metal Science and Heat Treatment*. 1968; 10(3).
 23. Kobasko NI, Aronov MA, Ichitani K, Hasegawa M, Noguchi K. High compressive residual stresses in through hardened steel parts as a function of Biot number. In a Book “Recent Advances in Fluid Mechanics, Heat & Mass Transfer and Biology”. WSEAS Press, Harvard, 2012, 36-40.
 24. Tolubinsky VI. Teploobmen pri kipenii. Heat transfer at boiling. *Naukova Dumka*, Kyiv, Ukraine, 1980, 320.
 25. Kobasko NI. Isothermal Method for Hardening of High Carbon Steels and Irons. UA Patent No. 109935, 2015.
 26. Kobasko N. Austempering processes that are performed via cold liquids. Lambert Academic Publishing, Germany, 2019, 107. ISBN: 978-620-0-11330-6.
 27. Kondrat'ev GM. Teplovye Izmereniya (Thermal measurements), Mashgiz, Moscow, 1957.
 28. Kobasko N, Guseynov Sh, Rimshans J. Core Hardness and Microstructure Prediction in Any Steel Part. Lambert Academic Publishing, Germany, 2019, 94. ISBN: 978-613-9-94751-5.
 29. Totten GE, Bates CE, Clinton MA. Handbook of Quenchants and Quenching Technology. ASM International, Materials Park, OH, USA, 1993, 507.
 30. Mukhina MP, Kobasko NI, Gordeeva LV. Hardening of Structural Steels in Cooling Media Based on Chlorides. *Metal Science and Heat Treatment*. 1989; 31(9):677-682.
 31. Shevchenko SYu, Smirnov AE, Kirillov IV, Kupriakova NA. Investigation of hardening during cooling in gas media. *MiTOM*. 2016; 734(8):15-19. ISSN: 0026 – 0819.
 32. Boyer HE. (Ed). Atlas of Isothermal Transformation and Cooling Transformation Diagrams. American Society for Metals. Metals Park. Ohio 44073. USA. 422.
 33. Kobasko NI, Liscic B. Liscic/Petrofer probe to investigate real industrial hardening processes and some fundamentals during quenching of steel parts in liquid media. *EUREKA: Physics and Engineering*, 2017; 6:48-56.
 34. Bhadeshia HKDH. Bainite in Steels: Theory and Practice. 3rd edn. New York: CRC Press Money Publishing, 616..
 35. Kobasko NI, USA Patent US 6,364,974 B2, Quenching apparatus and method for hardening steel parts. Assignee: IQ Technologies, Inc Appl. 09/551,082. Filed 18.04.2000, 2002. Available at: <http://patents.com/us-6364974.html>